DOI: 10.1021/ma100565s

Macromolecules
ARTICLE

Bulk Streaming Potential in Poly(acrylic acid)/Poly(acrylamide) Hydrogels

Andrea Fiumefreddo[†,‡] and Marcel Utz*[,†,‡,§]

[†]*Center for Microsystems for the Life Sciences,* [‡]*Department of Mechanical and Aerospace Engineering, and* [§]*Department of Chemistry, University of Virginia, Charlottesville, Virginia 22904*

Received March 16, 2010; Revised Manuscript Received May 18, 2010

ABSTRACT: The streaming potential through poly(acrylic acid)-*co*-acrylamide polymer hydrogel (poly-AA-*co*-AM) membranes has been measured as a function of gel composition and ionic strength of the solvent. Polyelectrolyte hydrogels have important potential applications as mechanical transducers. The current work aims at providing a quantitative basis to understanding the relationship between gel composition and structure and the electromechanical coupling properties. The streaming potential increases in magnitude with the spatial density of negative charges in the gel, up to a saturation point where the density of charges on the polymer backbone becomes comparable to the salt concentration of the equilibrating solution. A simple theory of coupled charge and solvent transport based on the model proposed by de Gennes et al. [*Europhys. Lett.* **2000**, *50*, 513] quantitatively accounts for the observed effects.

Introduction

The response of polyelectrolyte hydrogels to environmental influences, such as changes in pH and temperature, has received sustained scientific interest. Deformation of a polyelectrolyte gel subjected to an electric field was first reported by Tanaka et al.[1] The electromechanical properties of such gels have since been explored in view of a wide range of applications,[2−4] including fuel cells, environmental filtration, and artificial muscles.[5−12] Most work has been devoted to actuators, which convert electrical signals into a mechanical response. By contrast, the reverse effect, where the gel is exposed to a mechanical stress which then results in a measurable electrical field, has not been studied as thoroughly. Hydrogels are promising for tactile sensing in biomedical applications due to their compliance and biocompatibility. However, quantitative understanding of the electromechanical transduction process is a prerequisite for application development. In the present paper, we report systematic measurements of the streaming potential across polyelectrolyte gel membranes in contact with an electrolyte, with the goal to establish the relationship between gel structure and electromechanical properties.

The streaming potential, i.e., the electrochemical potential that develops in response to fluid transport, has been used extensively for the surface characterization of polymer thin films and membranes,[13−16] fibers,[17] capillaries,[18] and microfluidic channels.[19] In these measurements, the flow is tangential to the polymer surface under study. By contrast, the bulk streaming potential is measured by forcing solvent flow through the thickness of a porous membrane.[20] The bulk streaming potential has been studied in ion-exchange membranes[21] and polymer electrolytes for fuel cell applications[22,23] but not, to our knowledge, in poly(acrylamide/acrylic acid) gels. This is surprising in light of how much attention these systems have received in the context of polymer actuators.

As detailed in the remainder of this paper, we have measured the bulk streaming potential in poly(acrylic acid)/poly(acrylamide) hydrogels as a function of both solution salt concentration and the acrylic acid (AA) to acrylamide (AM) ratio, which amounts to a systematic variation of the spatial density of negative charges on the polymer backbone. We found the streaming potential to be proportional to the applied pressure, with a proportionality coefficient that increases systematically with the acrylic acid content and decreases with the salt concentration of the solution. The results are well represented by de Gennes' theory of ion transport through membranes,[24] which we generalized to incorporate the effect of solvent salt content. These results complement a recent study[25] of the response of similar gels to direct loading with a solid indentor. As discussed below, the electromechanical response is similar, but not identical, in the two cases.

*Corresponding author. E-mail: mu3q@virginia.edu.

Experimental Methods

Materials. Copolymer gels were synthesized[25] from acrylamide (AM) (99.0% electrophoresis grade, Aldrich) and acrylic acid (AA) (purum 99.0%, Fluka) by free radical polymerization with *N*,*N*′-methylenebis(acrylamide) (nBisA) (>98.0%, Sigma) as the cross-linking agent, using 2,2-dimethoxy-2-phenylacetophenone (DMPA) (Sigma-Aldrich) as a photoinitiator and dimethyl sulfoxide (DMSO) (>99.9%, Sigma-Aldrich) and potassium biphthalate sodium hydroxide buffers (Fisher) at pH 4.00 ± 0.02 (0.05 M) and pH 5 ± 0.02 (0.05 M) as solvents. The electrolyte solution was composed of deionized ultrafiltered (DIUF) water (Fisher) and 5 M sodium chloride (Sigma-Aldrich). All reagents and solutions were degassed prior to use by bubbling with dry nitrogen (GTS, 99.9%).

Gel Synthesis. Stock solution A was prepared from 0.03845 g of DMPA in 2.0 mL of DMSO. The solution was sonicated until all DMPA dissolved. This solution was always covered and kept in the dark. A second stock solution B contained the monomers and cross-linking agent, as described in Table 1. The cross-link density was selected to ensure mechanical properties amenable to streaming potential measurements. While weakly cross-linked gels were not strong enough to sustain substantial pressure gradients, too much cross-linking produced brittle gels that fractured upon insertion into the apparatus. A molar ratio of 0.57% cross-linker to total monomer was found to produce gels with satisfactory properties. Stock solution B was prepared by mixing AA and AM in varying amounts (0% AA to 100% AA by mole fraction) with the 98.5 mg of nBisA in the pH 4 buffer. The total monomer concentration in this solution varied slightly about 3.9 M, as indicated in Table 1. 0.2 mL of A was then mixed with 2 mL of B, sonicated for 2 min, and filled into a

 Published on Web 06/14/2010

Table 1. Composition of Samples Used in Experiments in Terms of Exact Measurements for the Stock Solution Containing the Monomers and Cross-Linker as Well as Total Concentrations in the Gel's Final Form

sample	nBisA (mM)	AA (M)	AM (M)	monomer (M)	AM (%)
1	22.35	0.00	3.86	3.86	0
2	22.38	0.06	3.78	3.84	1.5
3	22.37	0.12	3.72	3.85	3.0
4	22.35	0.27	3.58	3.85	6.5
5	22.32	0.53	3.33	3.86	13
6	22.26	1.02	2.86	3.88	25
7	22.20	1.46	2.44	3.90	36
8	22.11	2.02	1.91	3.93	50
9	22.00	3.01	0.94	3.95	75
10	21.88	3.97	0.00	3.97	100

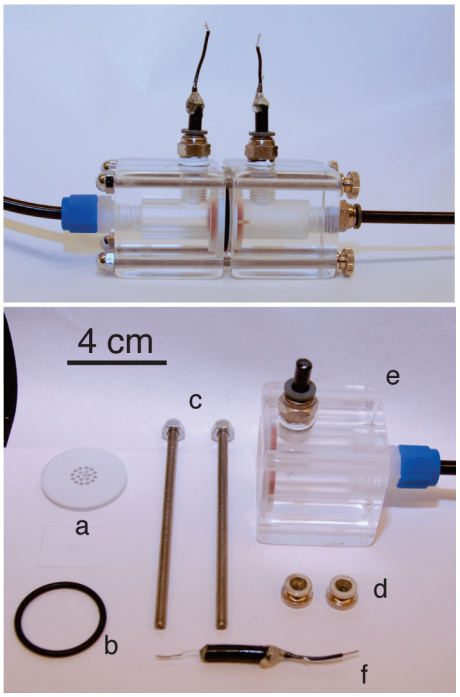

Figure 1. Pressure cell assembly: (a) sieve plate, (b) O-ring, (c) steel rods to connect half-cells, (d) acrylic block cell, (e) cell-tightening screws, and (f) electrode.

PDMS mold of 5 mm thickness held between two microscope glass slides. Polymerization was initiated by irradiation at 365 nm with a UV lamp (Spectroline Model ENF-260C, Spectronics Corp., Westbury, NY) for 10 min. The resulting gels were equilibrated for at least 7 days at room temperature in a large excess of solutions of 0.03, 0.01, or 0.003 M NaCl and pH 5 buffer (0.05 M) at a 9:1 volume ratio, with salt concentrations of 0.032, 0.014, and 0.00797 M, respectively. Swelling ratios were determined by weighing the gels after gentle drying with a paper tissue (Kimberly-Clark).

Apparatus. An apparatus consisting of two liquid chambers separated by the hydrogel sample was used for streaming potential measurements, as shown in Figure 1.[22] A closed-loop electronic pressure controller (Type 640A, MKS Instruments, Inc.) was used in conjunction with a digital power supply and readout (Model PR4000A, MKS Instruments, Inc.) to control the pressure in the upstream chamber. Compressed nitrogen gas (GTS, 99.9% purity) was used as primary pressure source. The downstream chamber was kept at ambient pressure. Each chamber contained an inlet for a silver−silver chloride (Ag/AgCl) electrode. The interface between the chambers was composed of two polypropylene sieve plates, each pierced with 2 mm holes in a concentric circle pattern, a rubber O-ring with thickness approximately equal to that of the gel sample, and the sample itself. Prior to insertion into the apparatus, the samples were covered with a thin sheet of polypropylene with pin-point-sized piercings on either side to prevent damage.

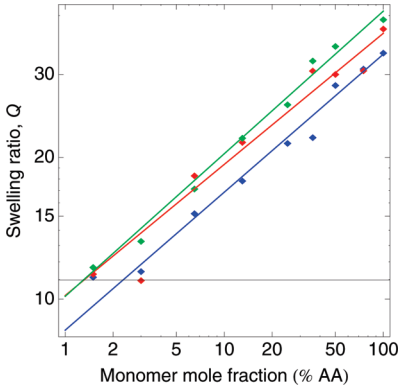

Figure 2. Swelling ratio versus the mole fraction of acrylic acid in AA-*co*-AM gels equilibrated in pH 5 buffer at three different salt concentrations. Power law fit for curves in the form ax^b. Blue: 0.032 M (a = 8.59, b = 0.293). Red: 0.014 M (a = 10.18, b = 0.278). Green: 0.00797 M (a = 10.14, b = 0.303).

Measurement Procedures. A harmonically modulated pressure at a frequency of 0.01 Hz, with amplitudes ranging from 0 to 13.8 kPa, was applied to one side of the cell while the other remained open to the atmosphere. A silver/silver chloride wire electrode was placed in the solution on either side of the gel membrane. Prior to every measurement, the electrodes on the two sides of the hydrogel membrane were equilibrated by short-circuiting for at least 24 h.[26] It was found that mechanically securing the electrodes and the membrane was critical for stable measurements. Voltages were measured with a Gamry 600 potentiostat in open-circuit potential mode, and the voltage data were saved to a file at a rate of 100 samples/min. All measurements were made with the same electrolyte that the gels were equilibrated in.

Results and Discussion

Swelling. The swelling ratio, Q, was determined from the known initial swelling degree at synthesis, Q_0, and the mass of the gel following equilibration with the solvent, using the expression[27]

$$Q(t) = Q_0 \frac{m(t)}{m_0} \tag{1}$$

where $m(t)$ is the mass of the swollen gel after equilibration at time t, and m_0 and Q_0 are the initial mass and swelling ratio following UV polymerization, respectively. All gels had similar initial swelling ratios around 3.7.

The swelling ratio, together with the initial acrylic acid content, determines the final spatial density of ionizable carboxylic groups in the equilibrated gel. As Figure 2 shows, the swelling ratio increases with the acrylic acid content and decreases with the salt concentration of the solvent solution. The data are well represented by a power law with an exponent of 0.29 ± 0.02.

Negative Charge and Cross-Link Densities. The spatial densities of ionizable groups ρ_- and cross-link points ρ_{cr} are given by

$$\rho_- = \frac{\rho_{gel}}{Q} \frac{n_{AA}}{n_{AA}M_{AA} + n_{AM}M_{AM}} \tag{2}$$

$$\rho_{cr} = \frac{\rho_{gel}}{Q} \frac{n_{cr}}{n_{AA}M_{AA} + n_{AM}M_{AM}} \tag{3}$$

where n_{AA} and n_{cr} are the molar amounts of acrylic acid monomer and cross-linker, respectively, M_{AA} and M_{AM} are

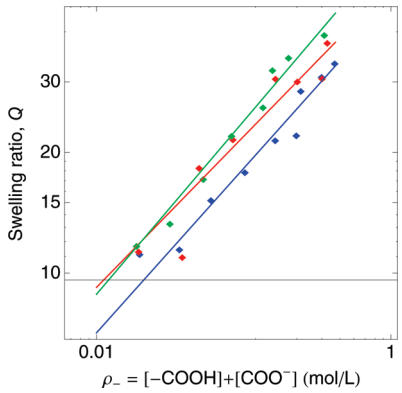

Figure 3. Swelling ratio versus the density of carboxylic acid groups $\rho_- = [COOH] + [COO^-]$ in AA-*co*-AM gels equilibrated in pH 5 buffer solution at three different salt concentrations. Power law fit for curves in the form ax^b. Blue: 0.032 M (a = 46.95, b = 0.41). Red: 0.014 M (a = 52.21, b = 0.38). Green: 0.00797 M (a = 64.75, b = 0.43).

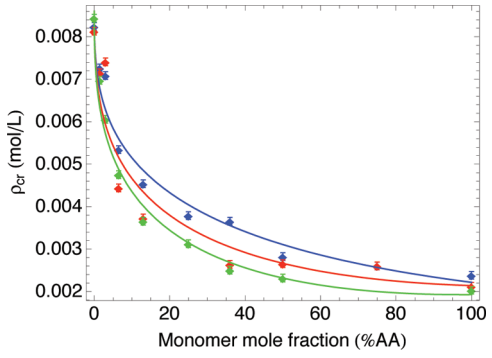

Figure 4. Density of cross-linker in gel as varying with acrylic acid monomer mole fraction percentage.

the molar mass of acrylic acid and acrylamide, and Q represents the swelling ratio as defined in eq 1. In these expressions, the mass of the cross-linker is neglected, and we assume $\rho_{gel} = 1000\ kg/m^3$. The density of cross-links decreases with increasing acrylic acid content as a consequence of the increase in swelling ratio (Figure 4).

By contrast, the density of carboxylic groups ρ_- increases with the acrylic acid content. However, the increase is less than linear due to the simultaneous increase in swelling, as shown in Figure 5.

Streaming Potential. Figure 6 shows the time-modulated pressure that was applied to measure the streaming potential, along with a typical voltage readout between the upstream and downstream chamber Ag/AgCl electrodes. The potential difference follows the pressure difference with a 180° phase shift. The relationship between pressure and potential is highly linear. This was verified by measuring the output amplitude as a function of input amplitude, as well as by Fourier analysis of the input and output signals, which were free from higher harmonics to within experimental noise.

In principle, the measured potential difference would have to be corrected for the pressure dependence of the electrode potential. For silver−silver chloride electrodes, this amounts to 0.16 μV/kPa,[28,29] resulting in a correction of the order of 2 μV for the pressure range used here. This is negligibly small in the present context, and we have therefore not corrected our data for this effect.

Experimentally determined streaming potential coefficients are shown in Figure 7, both as a function of acrylic acid/acrylamide composition (Figure 7A) and as a function

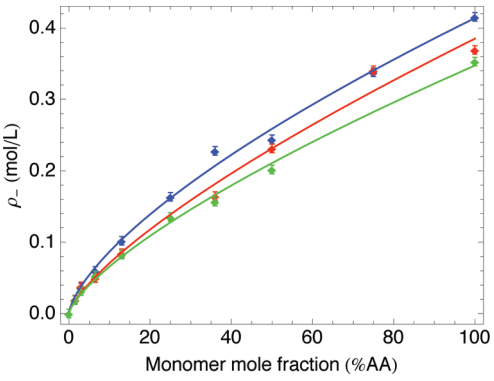

Figure 5. Density of ionizable groups $\rho_- = [COO^-] + [COOH]$ vs acrylic acid content. The error source lies in the uncertainty associated with the swelling degree measurements.[2]

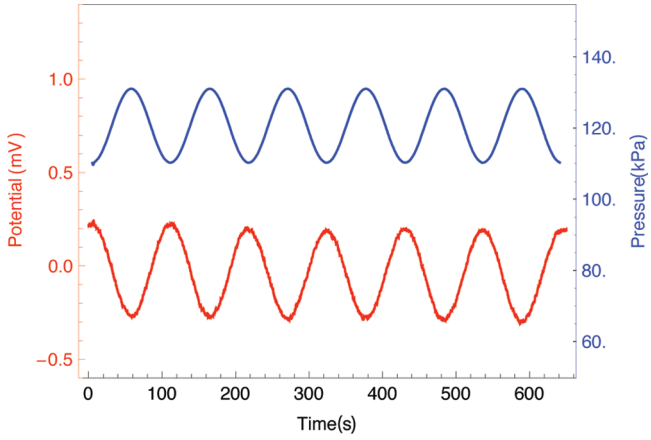

Figure 6. Typical pressure input (top curve) and resulting streaming potential response (bottom curve). These data were collected from a gel containing 3% monomer mole fraction AA in 0.0033 M NaCl.

of the resulting spatial density of ionizable groups after swelling (Figure 7B). Measurements have been carried out at three different solution salt concentrations, as indicated in the figures. The streaming potential coefficient increases with increasing acrylic acid content, as a consequence of the resulting higher spatial density of ionizable groups. By contrast, higher solution salt concentration clearly leads to a screening effect, lowering the observed streaming potential.

These trends can be rationalized quantitatively on the basis of a theory developed by de Gennes[24] for the electromechanical coupling in Nafion-type membranes. Only a straightforward extension is required to include the effects of solvent salt content. For the streaming potential measurement, the charge flux normal to the membrane j, and the solvent flux q must be considered. These fluxes are induced by the electric field, $\nabla\phi$, and the pressure gradient, ∇P, respectively. Assume that the x-direction is perpendicular to the membrane such that $-\nabla P = -\partial P/\partial x$. Following Onsager, the current density j and volume flux q are then given by

$$j = \sigma\nabla\phi - L_{12}\nabla P \tag{4}$$

$$q = L_{21}\nabla\phi - K\nabla P \tag{5}$$

where σ is the membrane conductance and K is the Darcy permeability, which depends on both the material (e.g., pore size) and the fluid (e.g., viscosity).[30,31] For zero potential

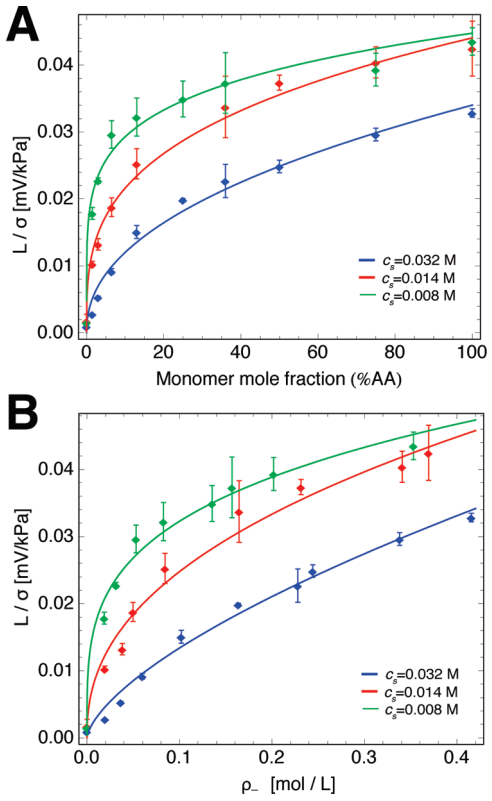

Figure 7. Streaming potential coefficient L/σ as a function of acrylic acid/acrylamide ratio (A) and as a function of spatial density of acrylic acid groups ρ_- (B). Three different solution salt concentrations c_s have been used, as indicated in the figures. The solid lines are power law fits to the data and are meant as guides to the eye.

difference, one obtains

$$K = \frac{J_q h}{A\Delta P} \tag{6}$$

where h is the thickness of the membrane, A the cross-sectional area, $J_q = qA$ the volumetric flow rate, ΔP the applied pressure difference, and $\partial P/\partial x = \Delta P/h$. Following de Gennes,[24] K can be expressed using a characteristic pore size of the gel, d, volume fraction of solvent, ψ, and its viscosity, η, as

$$K = \psi \frac{d^2}{\eta} \tag{7}$$

Because of Onsager's reciprocal relation, we have $L = L_{12} = L_{21}$ in eqs 4 and 5. While measuring the streaming potential, no net current is allowed to flow ($j = 0$). Equation 4 then yields for the streaming potential coefficient

$$\frac{L}{\sigma} = \frac{\nabla\phi}{\nabla P} = \frac{\Delta\phi}{\Delta P} \tag{8}$$

The conductivity σ can be estimated from number density of mobile ions of type k, n_k, and their frictional coefficient ζ_k as[24]

$$\sigma = \sum_k \frac{n_k e^2}{\zeta_k} \tag{9}$$

where e is the elementary charge and all ions have been assumed to be monovalent. In order to estimate the electromechanical coupling coefficient, L, we assume that the transported ions in the system carry with their charge ($n_k e$) a hydrodynamic volume, w_k, due to hydration and attribute to them a friction coefficient ζ_k. In the absence of a pressure gradient, the solvent volume flux q in eq 5 becomes

$$q = L\nabla\phi = \nabla\phi \sum_k \frac{n_k e}{\zeta_k} w_k \tag{10}$$

where the hydrodynamic volume and friction coefficient are individual to each mobile ion constituent in the system.

For simplicity, we will assume a gel that contains dissociable groups (consisting of a fixed negative charge and a sodium ion) at concentration ρ_-, in equilibrium with a surrounding solution containing a sodium chloride electrolyte (at concentration c_s). The pH of the surrounding solution is assumed to be buffered at a fixed value.

Because of electroneutrality inside the gel, we have

$$[A^+] = \beta\rho_- + [B^-] \tag{11}$$

where $[A^+]$ and $[B^-]$ denote the concentrations of free positive and negative ions *within* the gel, and β is the degree of dissociation of the ionizable groups on the backbone. In the present case, $[A^+]$ and $[B^-]$ are dominated by the NaCl concentration in the solvent, with a minor contribution from the pH buffer. Because of the equilibrium of the gel with the surrounding solution, we have

$$[A^+][B^-] = {c_s}^2 \tag{12}$$

where c_s denotes the solution salt concentration. From these two equations, one obtains for $[Cl^-]$

$$[B^-] = \frac{1}{2}\left(\sqrt{\beta^2\rho_-^2 + 4c_s^2} - \beta\rho_-\right) \tag{13}$$

At moderate pH and realistic values for ρ_- and c_s, the conductivity of the gel is dominated by the mobility of the free ions. We can therefore write

$$\sigma = \frac{e^2}{\zeta}([A^+] + [B^-]) \tag{14}$$

where we have assumed a common friction coefficient ζ for simplicity. With the above relation, we obtain

$$\sigma = \frac{e^2}{\zeta}\sqrt{\beta^2\rho_-^2 + 4c_s^2} \tag{15}$$

which we insert into eq 10 to yield the streaming potential coefficient

$$\frac{L}{\sigma} = \frac{w}{e}\frac{\beta\rho_-}{\sqrt{\beta^2\rho_-^2 + 4c_s^2}} \tag{16}$$

where we have assumed the hydration volumes and friction coefficients to be equal for both the positive and negative free ions.

Figure 8 shows the streaming potential data on a doubly logarithmic scale, overlaid with a fit of eq 16 on the data. The only two fitting parameters are the dissociation degree, β, and the prefactor, w/e, whose best-fit values are $w/e = 0.046 \pm 0.01$ mV/kPa and $\beta = 0.23 \pm 0.05$. The logarithmic scale clearly reveals the trend toward saturation with increasing negative

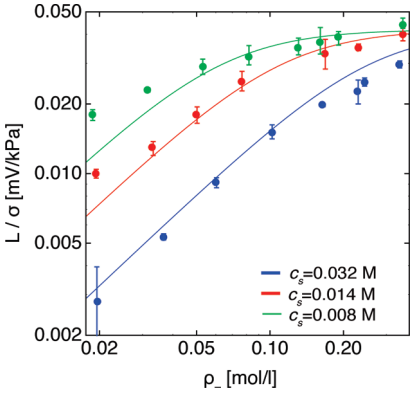

Figure 8. Log−log plot of streaming potential coefficient versus negative charge density within the gel at three salt concentrations dependent upon the combined concentration of sodium chloride and pH 5 buffer. The lines represent the least-squares fit of eq 16.

charge density in the gel. The saturation point depends on the ionic strength of the solvent: the streaming potential coefficient increases with the negative charge density on the polymer backbone up to a point where $\beta\rho_- \approx c_s$ and then saturates. In other words, the streaming potential coefficient is limited by the ionic strength of the surrounding medium. Particularly for systems intended to operate in a physiological context, this is an important finding.

While the model shown in Figure 8 largely agrees with the data within experimental error, the fit is not perfect. At low salt concentration and low negative charge concentration, the model systematically underpredicts the streaming potential. We believe that this is a consequence of oversimplification of the model. While the friction coefficients of Cl^- and Na^+ are known to lie within 30% of each other,[32] there is no experimental justification for our assumption of a common value for the hydration volume w. At the expense of introducing an additional fit parameter, a version of eq 16 that allows for two different values w_A and w_B can easily be derived. Using experimental values[32] for the friction coefficients of Cl^- and Na^+ at the same time, we indeed found the quality of fit to improve somewhat, but not significantly enough to justify the introduction of an additional parameter. It is known that the dissociation degree of poly(acrylic acid) systems depends on the spatial density of acrylic acid groups.[25,33] This would lead to β depending slightly on ρ_-, which is not reflected in the model. Finally, the activity coefficients of the free ions have implicitly been set to unity. In spite of these limitations, however, the model seems to capture the essential physics of the problem.

It is interesting to compare the streaming potential data obtained here to the results of a study recently completed in our laboratory,[25] where the gels were subjected to direct mechanical indentation with a rigid spherical body, instead of exposure to a pressurized electrolyte. The gels used in ref 25 had somewhat higher cross-link densities than the ones studied here, and they were equilibrated at lower salt concentration. However, the negative charge densities were comparable. Both the streaming potential and the electromechanical response to indentation increase systematically with the density of negative charges on the polymer backbone. At a given charge density, the electromechanical response measured by indentation was about a factor of 3 smaller than the streaming potential coefficient. Nevertheless, the similarity of the magnitude of the effect suggests that both the response to a liquid pressure and indentation with a solid are based on the similar physical processes.

Conclusions

The streaming potential in a sequence of acrylamide/acrylic acid hydrogels has been measured as a function of both gel composition and salt concentration. The potential increases with the spatial density of fixed negative charges in the polymer gel and decreases with the salt content of the surrounding solution. Streaming potential coefficients in the range of 2 to about 40 nV/Pa were observed. In order to produce easily observable electrical signals in the millivolt range, these gels have therefore to be exposed to kilopascal level pressures. The increase with charge density saturates when the latter becomes comparable to the salt concentration of the surrounding medium. Under conditions of fixed ionic strength (for example, in a physiological context), this dictates the optimal charge density for maximum electromechanical coupling. The experimentally observed behavior is predicted quantitatively by a simple extension of the theory developed by de Gennes for the electromechanical properties of Nafion-type ionic polymer systems. Efforts to combine this theory with recently developed continuum models for the deformation and swelling of gels in the presence of mechanical loads[34,35] are currently underway in our laboratory and will be reported at a later occasion.

Acknowledgment. We are grateful to Ms. Katsiaryna Prudnikova for help with the synthesis of the samples. Helpful discussions with Prof. Andrei Dobrynin are gratefully asckowledged. This work was supported by the US National Science Foundation under Grants DMR-0647790 and CHE-0809795.

References and Notes

(1) Tanaka, T.; Nishio, I.; Sun, S.; Ueno-Nishio, S. *Science* **1982**, *218*, 467–469.
(2) Wallmersperger, T.; Kroplin, B.; Gulch, R. *Mech. Mater.* **2004**, *36*, 411–420.
(3) Yamaue, T.; Mukai, H.; Asaka, K.; Doi, M. *Macromolecules* **2005**, *38*, 1349–1356.
(4) Yao, L.; Krause, S. *Macromolecules* **2003**, *36*, 2055–2065.
(5) Okada, T.; Kjelstrup-Ratkje, S.; Moller-Holst, S.; Jerdal, L.; Friestad, K.; Xie, G.; Holmen, R. *J. Membr. Sci.* **1996**, *111*, 159–167.
(6) Trivuitkasem, P.; Ostvold, T. *Electrochim. Acta* **1980**, *25*, 171–178.
(7) Garrido, J. *J. Electrochem. Soc.* **2003**, *150*, E567–E570.
(8) Raynauld, J.; Laviolette, J. *J. Neurosci. Methods* **1987**, *19*, 249–255.
(9) Khedr, M.; Abd El Haleem, S.; Baraka, A. *J. Electroanal. Chem.* **1985**, *182*, 157–167.
(10) Li, W.; Zhao, H.; Teasdale, P.; John, R.; Zhang, S. *React. Funct. Polym.* **2002**, *52*, 31–41.
(11) Kim, S.; Kim, J.; Park, I.; S., J.; Kim; Lee, S.; Lee, T.; Kim, S. *Smart Mater. Struct.* **2005**, *14*, 511–514.
(12) Shahinpoor, M.; Bar-Cohen, Y.; Simpson, J.; Smith, J. *Smart Mater. Struct.* **1998**, *7*, R15–R30.
(13) Adamson, A.; Gast, A. *Physical Chemistry of Surfaces*; Wiley: New York, 1990.
(14) Van Wagenen, R.; Coleman, D.; King, R.; Triolo, P.; Brostrom, L.; Smith, L.; Gregonis, D.; Andrade, J. *J. Colloid Interface Sci.* **1981**, *84*, 155–162.
(15) Elimelech, M.; Chen, W.; Waypa, J. *Desalination* **1994**, *95*, 269–286.
(16) Möckel, D.; Staude, E.; Dal-Cin, M.; Darcovich, K.; Guiver, M. *J. Membr. Sci.* **1998**, *145*, 211–222.
(17) Stana-Kleinschek, K.; Ribitsch, V. *Colloids Surf., A* **1998**, *140*, 127–138.
(18) Wang, T.; Hartwick, R. *J. Chromatogr. A* **1992**, *594*, 325–334.
(19) Kirby, B.; Hasselbrink, E. *Electrophoresis* **2004**, *25*, 203–213.
(20) Toyoshima, Y.; Nozaki, H. *J. Phys. Chem.* **1969**, *73*, 2134–2141.
(21) Trivijitkasem, P.; Østvold, T. *Electrochim. Acta* **1980**, *25*, 171–178.
(22) Xie, G.; Okada, T. *J. Electrochem. Soc.* **1995**, *142*, 3057–3061.
(23) Pivovar, B. *Polymer* **2006**, *47*, 4194–4202.
(24) de Gennes, P.; Okumaura, K.; Shahinpoor, M.; Kim, K. *Europhys. Lett.* **2000**, *50*, 513–518.

(25) Prudnikova, K.; Utz, M. *Macromolecules* **2010**, *43*, 511–517.
(26) Wilbert, M.; Delagah, S.; Pellegrino, J. *J. Membr. Sci.* **1999**, *161*, 247–261.
(27) The cross-linker, nBisA, was not accounted for since its contribution is negligible in comparison to the other components.
(28) Fievet, P.; Sbai, M.; Szymczyk, A. *J. Membr. Sci.* **2005**, *264*, 1–12.
(29) Spiegler, K. *Desalination* **1974**, *15*, 135–140.
(30) Lee, S.; Lee, L. *Encyclopedia of Chemical Processing*; CRC Press: Boca Raton, FL, 2005.
(31) Clarke, J.; Marinsky, J.; Juda, W.; Rosenberg, N.; Alexander, S. *J. Phys. Chem.* **1952**, *56*, 100–105.
(32) Koneshan, S.; Rasaiah, J.; Lynden-Bell, R.; Lees, S. *J. Phys. Chem. B* **1998**, *102*, 4193–4204.
(33) Schosseler, F.; Ilmain, F.; Candau, S. *Macromolecules* **1991**, *24*, 225–234.
(34) Hong, W.; Zhao, X.; Zhou, J.; Suo, Z. *J. Mech. Phys. Solids* **2008**, *56*, 1779–1793.
(35) Hong, W.; Liu, Z.; Suo, Z. *Int. J. Solids Struct.* **2009**, *46*, 3282–3289.